X-Band Uplink Technology Demonstration At DSS-13

J. G. Meeker and C. T. Timpe
Telecommunications Systems Section

This article reports the status of the X-band uplink development program from a systems' viewpoint.

The hardware, designed and built under the program, is now in place at DSS-13. System stability testing is underway.

An X-band receive capability is being implemented on both the Galileo and the Venus Radar Mapper spacecraft. Experiments will be conducted that will serve both to demonstrate the capabilities of the X-band uplink system and to enhance science objectives on those missions. These objectives are briefly described.

I. Introduction

The DSN undertook a phased development program in 1979, under RTOP 64, to add an X-band uplink capability to the deep space network. The first phase was to design and build highly stable ground station subsystems for installation and checkout at DSS-13. A second phase was to arrange a flight demonstration of a complete X-band uplink system to verify predicted performance in the space environment.

In order to plan and coordinate the activities, a systems work unit was established. Under it, various tasks were accomplished, utilizing a design team representing the various hardware subsystems, space environment disciplines, and the user community. The main efforts were directed towards the following tasks:

(1) Quantifying the requirements imposed on the overall system by potential users of the X-band uplink, particularly in the navigation and radio science areas.

(2) Establishing error budgets for the telecom functions of telemetry, ranging and Doppler, including error estimates, with tolerances, for ground and spacecraft hardware, and the natural media effects due to the troposphere and interplanetary and ionospheric charged particles.

(3) Maintaining extensive liaison with NASA flight projects to develop mutually beneficial X-band uplink experiments.

(4) Preparing an Experiment Requirements Document, defining a flight demonstration of the X-band uplink, including preparatory ground testing and inflight calibrations as well as experiment sequences.

Much of the early systems work was summarized in TDA Progress Report 42-62 (Ref. 1).

Subsequently, the NASA spacecraft of the ISPM mission, which was initially to have carried the X-band uplink demonstration experiment, was cancelled. This report tells of the developments which have taken place since then, including the status of DSS-13 X-band uplink activities and plans of the DSN now to support X-band uplink operations on the Galileo and Venus Radar Mapper missions.

II. Status of X-Band Uplink Activities at DSS-13

A. Hardware Status

The ground station hardware (Ref. 2) has been built and tested at the subsystem level, and is now installed at DSS-13. Included are the following subsystems:

(1) The X-band uplink exciter, X/X and X/S Doppler extractors and mixers and test signal translators which coherently translate the X-uplink frequency to X- and S-downlink frequencies for in-station tests.

(2) The 20-kW klystron power amplifier, with buffer amplifier driver, complete with power supplies, controller and protective circuitry.

(3) A new microwave antenna feed design to accommodate S- and X-band uplinks and downlinks.

(4) An X-band diplexer, specially designed to minimize noise temperature contributions.

(5) Block III receiver modifications. In order to realize the potential advantages of the X-band uplink in reducing phase jitter due to charged particle variations in the solar wind and the ionosphere, the station will use a Hydrogen-maser timing reference and will incorporate a temperature-controlled Multi-mission Receiver (MMR) front end. Concepts consistent with unattended operations have also been employed.

The components that have been redesigned in the X-band uplink R & D effort, and are now in place at DSS-13, are indicated in the block diagrams. Fig. 1 shows the station as it would be configured to support an X-band demonstration with the Galileo mission, while Figs. 2 and 3 show the hardware in more functional detail for the X-band uplink/X-band downlink and X-band uplink/S-band downlink paths respectively.

B. DSS-13 System Test Status

Individual subsystems were checked out prior to installation at DSS-13 to verify that they met their design specifications.

In addition, a stepwise test plan was formulated to evaluate the total X-band uplink system. The approach emphasizes stability tests as the most informative. The testing is currently underway and will continue through 1984. The test sequence is as follows.

1. Baseline exciter subsystem stability. Exciter subsystem stability tests will serve as the baseline. Special tests were conducted prior to installation at DSS-13, in the Interim Frequency Standards Test Facility, using laboratory Hydrogen-masers as frequency references. Phase stability was measured at the X-band uplink frequency and at the downlink X- and S-band frequencies coherently derived from the uplink using the test signal translators that are part of the exciter subsystem. The phase data was processed to yield a square root Allan variance record versus sampling time.

The results of these measurements are encouraging. Fig. 4 shows a typical plot of the X-band uplink frequency stability over sampling times from 1 to over 20,000 seconds. The measurements have established that these exciter subsystem elements operate within the stability bounds specified for their design. Typical $(\Delta f/f)$ values below 3 parts in 10^{-15} were obtained for integration times over 1000 seconds.

2. X-band uplink stability at DSS-13. The exciter stability measurements are being repeated at the station at this writing. Because of the hardware's location in the antenna feedcone, a portable, highly stable microprocessor data system had to be designed for these in situ measurements. This has been built and tested, verifying an acceptably close match in stability to the laboratory instrumentation described previously.

The uplink frequency stability measurements will next be extended to various points moving progressively from the exciter to the buffer amplifier and the 20-kW klystron power amplifier. These measurements will identify additional noise increments added along the path to the antenna.

The measurements will be performed first by open loop, and then by closed feedback path back to the exciter from, for example, the output of the klystron power amplifier. The feedback loop has been included to compensate for relatively slow phase changes in subsystems that are especially subject to variations in ambient temperature. The loop should essentially clamp the phase's excursions to those of the exciter, and its success depends on the stability in the feedback path and the gain in the loop. Note that the loop time constant should be long enough to permit passage of command and ranging modulations.

3. **Receiver testing.** The next tests will bring in portions of the receiver. For these tests, downlink frequencies will be generated using the X-up/X-down and X-up/S-down frequency translators operating on a sample of the X-band uplink extracted via a directional coupler. The receiver frequencies would be reinserted in the downlink path, also via couplers, after being adjusted to the proper level. Stability measurements would be made at these RF frequencies down to the point where downconversion occurs. At this point, viz the outputs of the X- and S-band masers, the DSS-13 station configuration is representative of the configuration which will be implemented in the High Efficiency (HEF) operational stations, DSS-15, DSS-45 and DSS-65. Therefore, stability measurements made at DSS-13 at the maser output should also be representative of those expected at the operational stations. From this point, however, the configurations differ. The HEF stations, shown in Fig. 5, will route closed-loop data for radiometric measurements, such as Doppler, through conventional 34-m station hardware consisting of an X- to S-downconverter followed by a Standard Block III S-band receiver.

In the HEF stations a separate signal path will utilize the temperature-controlled and phase-calibrated Multimission Receiver (MMR) RF frontend. This path leads to an open-loop receiver within an Occultation Data Assembly (ODA) for use by radio scientists to collect data for further processing in experiments such as the extraction of Doppler signatures for gravitational wave searches to be conducted on the Galileo mission.

In contrast, DSS-13 will utilize only a closed-loop receiver at this time, but will enhance the Block III receiver performance by adding modifications. The receiver modifications consist of a MMR frontend and an upconverter/downconverter section prior to interfacing with a Standard Block III receiver. Figs. 1 and 5 compare the configurations at DSS-13 and the HEF stations respectively.

4. **Doppler stability tests at DSS-13.** The next step is to bring the entire closed-loop DSS-13 system into play in an end-to-end stability test. The most meaningful point in the system to make this test is felt to be the output of the Doppler mixer, at either the 5 MHz or 1 MHz bias frequency point. This measurement would involve all of the transmit and receive hardware at the station, except the antenna, and would be indicative of the system noise "floor" for the station components.

5. **Inflight demonstration.** The final test of system stability will be accomplished using an actual space mission. This will first occur during the Galileo flight and will bring into play the elements of the total system not available before, including the station antenna, the total spacecraft receive/transmit system, and the intervening media.

Emphasis in the initial inflight demonstration test would again be on two-way Doppler stability using DSS-13 and Galileo. In order to obtain the best achievable conditions, the experiment would be performed at Galileo's first opposition. This view period has two advantages from a stability standpoint. It would provide a "quiet" environment (nighttime viewing) and would occur while the spacecraft is still close to earth; hence, it would feature strong signal conditions. The test should, in effect, establish a new system noise "floor," but this time for the total end-to-end system, complete with spacecraft and media.

Subsequent X-band uplink technology demonstration sequences would test other telecommunications functions, such as commanding and two-way coherent telemetry.

C. Supporting Analysis: Doppler Error Source Modeling

As noted, end-to-end tests are planned during 1984 to measure the phase stability of the DSS-13 X-band uplink station configuration. Preceding this, an analysis task was undertaken to guide the interpretation of the test results. In it, equations were derived for the phase transfer functions relating the contributions of error sources in the system to various output points including the X-band and S-band biased Doppler mixer outputs. A follow-up task is recommended for the future. This will involve obtaining and assigning phase power spectra for the major phase error sources such as VCOs, frequency synthesizers, cables and the H-Maser reference so that accurate quantitative predictions can be made.

The first part of this analysis, the derivation of the transfer-function equations, has been completed and was reported in TDA Progress Report 42-76 (Ref. 3). It considered two modes. One, for station testing, uses a test signal translator (a zero-delay device) as an uplink/downlink turnaround device. The second configuration models a system with an actual spacecraft at a significant round trip light time from the DSN station. The results indicate that system tests at the station can be useful in localizing many of the phase errors contributed by the station hardware, but cannot accurately reflect the net Doppler error that will occur during actual spacecraft tracking. Aside from space environment factors, lack of fidelity in simulating real mission conditions is due to two main differences between test and flight conditions:

(1) The round-trip times between an uplink transmission and subsequent downlink reception in a mission cannot be simulated in station tests. Therefore, in the station tests, phase error sources that are common to both the

uplink signal and the Doppler extractor will be highly correlated because they are generated from the same reference. These errors will be largely cancelled out in a process such as the conventional two-way Doppler measurement, wherein a Doppler reference and an estimate of a received signal are subtracted. However, some errors that enter only one part of the system, such as the phase error contributions of the X-band and S-band receiver VCOs and frequency synthesizers (DCOs) will be accurately identified in station tests.

(2) Translator turnaround devices do not simulate the spacecraft transponder function accurately. A transponder produces a downlink frequency by multiplying the uplink frequency by the required turnaround ratio (880/749 for X/X and 240/749 for X/S). On the other hand, the test signal translators, used in the DSS-13 implementation, pick off samples of the uplink frequency from selectable points in the exciter power amplifier chain, and, using mixers, simply add or subtract coherent components required to give the downlink X- or S-frequencies. These components of the downlink frequencies are derived directly from the H-maser and DCO references and are not subject to errors generated in the power amplifier section of the uplink.

Thus, an X- or S-downlink generated by a test signal translator would have essentially the phase noise of the uplink. This is not the same as found in a downlink generated by a transponder where the phase noise would be multiplicatively increased by the X-down/X-up turnaround ratio (880/749) or decreased by the S-down/X-up turnaround ratio (240/749). This error, of course, could be eliminated by using a transponder for station tests, when available.

The above conclusions are somewhat qualitative, but do point out what to expect. Within the restrictions noted, the phase transfer functions derived in the analysis can be used to calculate quantitative results, given models for the phase power spectrum of each of the phase error sources.

III. Flight Projects

Both the Galileo and Venus Radar Mapper (VRM) projects have made decisions to fly an X-band uplink receive capability. Support had been provided to them prior to, and since, that time by the X-band uplink system work unit. This consisted primarily of technical inputs, such as estimates of radiometric accuracies using X-band vs S-band uplinks, and preliminary estimates of spacecraft hardware impacts and costs.

The X-band uplink sequences during these two missions will serve two purposes. On the one hand they will compare the performance of telecom functions using an X-band uplink system to the predictions of the systems design team. And they are expected to enhance selected flight project science objectives. Because science enhancements, rather than operational objectives, are primary for the X-band uplink on these two missions, present plans call for single string (nonredundant) implementations of X-band receive hardware on both spacecraft.

Fortuitously, the science experiments on Galileo and VRM present the opportunity to test an X-band uplink system in two different natural environments, using different station configurations. The gravitational wave search by Galileo will be conducted during solar oppositions (nighttime viewing) at long range. Doppler signatures with slow variations are expected. Open-loop receivers and extensive processing will be used.

The VRM gravity experiment, on the other hand, will necessarily be conducted during daytime viewing, with the sun-earth-probe angle often quite small. The Doppler signature in this experiment will be acquired using the closed-loop receiver and the sampling time will be short, i.e., typically 5 seconds.

Some of the objectives achievable through the use of an X-band uplink are summarized:

A. Galileo: X-Band Uplink Demonstration and Gravitational Wave Search

The objectives to be accomplished with the use of X-band uplink on the Galileo Orbiter can be included in three general areas. They are:

(1) A demonstration of improved performance in the various telecommunication links relative to S-band uplink.

(2) A demonstration of the DSN capability to maintain flight operations with operational, high-power X-band transmitters.

(3) A significant enhancement in the capability to perform the Gravitational Wave Experiment.

The plan for the demonstration of the advantages of X-band over S-band in telecommunication link performance is essentially the same as that which was previously intended for the ISPM U.S. spacecraft. Since these objectives were defined in detail in a previous report, (Timpe, C. T., private communication) they will be summarized here. The telecommunications

links on which improved performance will be demonstrated with X-band uplink are:

(1) Two-way coherent carrier tracking (Doppler stability).

(2) Command threshold.

(3) Two-way ranging.

(4) Two-way coherent telemetry data-rate.

The expected improvements in performance will result from the following two main factors:

(1) The net effect of a higher frequency on a one-way link (having the same size antennas, the same transmit power, and the same receive sensitivity) is a performance gain by a factor of approximately the square of the frequency ratio.

(2) The susceptibility of radiated energy to phase fluctuations induced by charged particles in the ionosphere, and in the interplanetary plasma decreases with higher frequencies.

The enhancement in the capability to perform the Gravitational Wave Experiment will result from the improvement in Doppler fractional frequency stability with X-band uplink. The system goal for overall fractional frequency stability on the ISPM ESA spacecraft with S-band uplink is 3×10^{-14} (the Allan variance on $\Delta f/f$ for a 1000 second time interval). The corresponding goal for Galileo with X-band uplink is 5×10^{-15}, or nearly an order of magnitude improvement. The two spacecraft will perform a joint gravitational wave (GW) search during their coincident solar opposition with the Earth in October of 1987. It is anticipated that GW activity, which may not be discernible in ISPM Doppler data by itself, may be very significant in verifying the existence of GW activity present in the Galileo Doppler data which can be time-correlated.

B. Venus Radar Mapper: X-Band Doppler Data for the VRM Gravity Experiment

In the past, S-band Doppler data have been the primary source for gravity field information. The experimenter relied strictly on what the navigation transponder produced. However, the major error in the S-band data is the effect from interplanetary media (plasma). The plasma produces amplitudes and frequencies that can be interpreted as gravity anomalies, when features near the resolution limits are being investigated.

With an X-band Doppler system these errors and high frequency noise can be reduced by a factor of 5 to 8 and much better resolution and statistical results on all features can be obtained. Presently, a gravity map of Venus has been extracted from the Pioneer Venus Orbiter data. A more detailed map will be obtained from Venus Radar Mapper data due to the X-band Doppler system and the smaller eccentricity of its orbit.

Gravity data are generally correlated with topographic results and then inferences are made on internal structure. For example, thickness of a crust or depth of isostatic adjustment are calculated at many areas. These in turn provide insight as to a general global structure. Also many topographic features can be classified by their gravity signatures, and, by using other geological evidence, inferences can be made on construction and age.

References

1. Komarek, T. A., Meeker, J. G., and Miller, R. L., ISPM X-Band Technology Demonstration. Part I, Overview, *TDA Progress Report 42-62*, Jet Propulsion Laboratory, Pasadena, California, January and February, 1981.

2. Hartop, R., Johns, C., and Kolbly R., X-Band Uplink Ground Systems Development, *Deep Space Network Progress Report 42-56*, Jet Propulsion Laboratory, Pasadena, California, January and February, 1980.

3. Koerner, M. A., Doppler Phase Transfer Functions for a System with an X-Band Uplink and X-Band and S-Band Downlinks, *TDA Progress Report 42-76*, Jet Propulsion Laboratory, Pasadena, California, October-December, 1983.

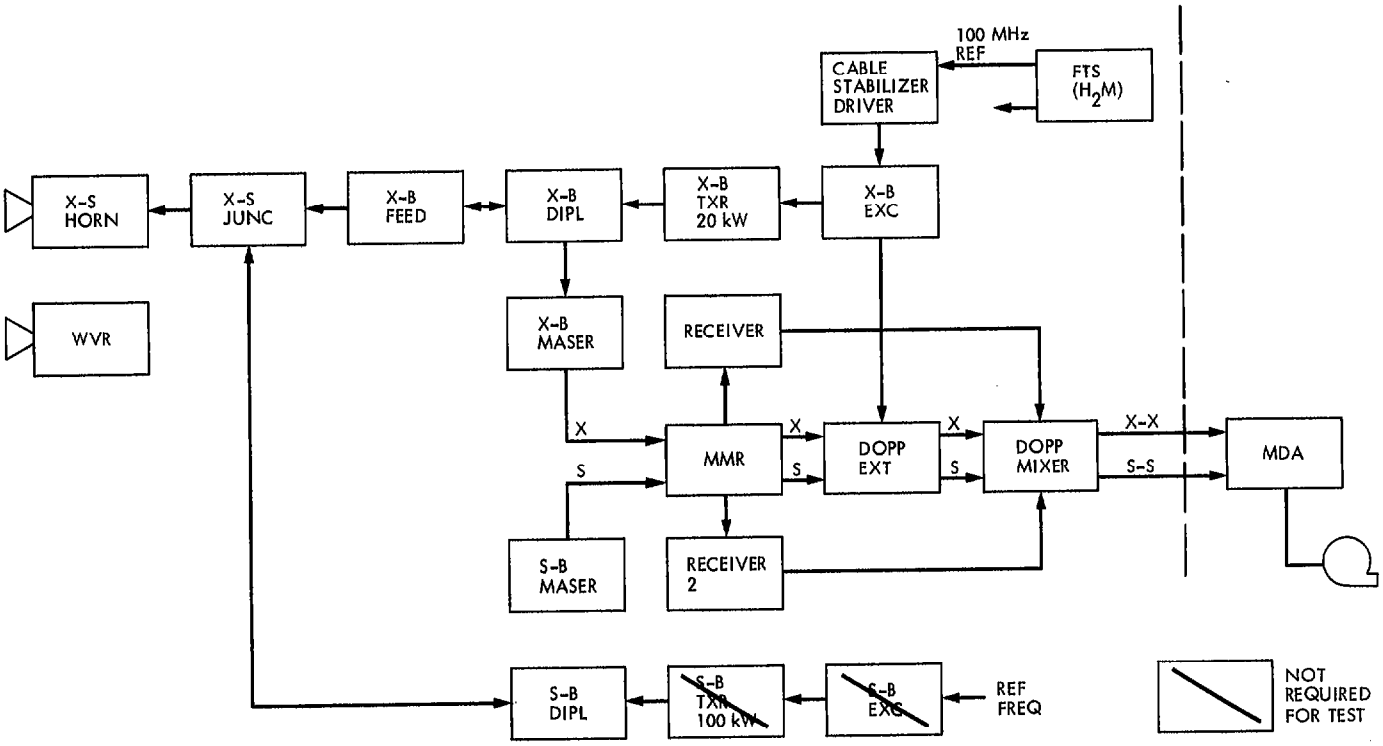

Fig. 1. X-band uplink functional configuration for DSS-13

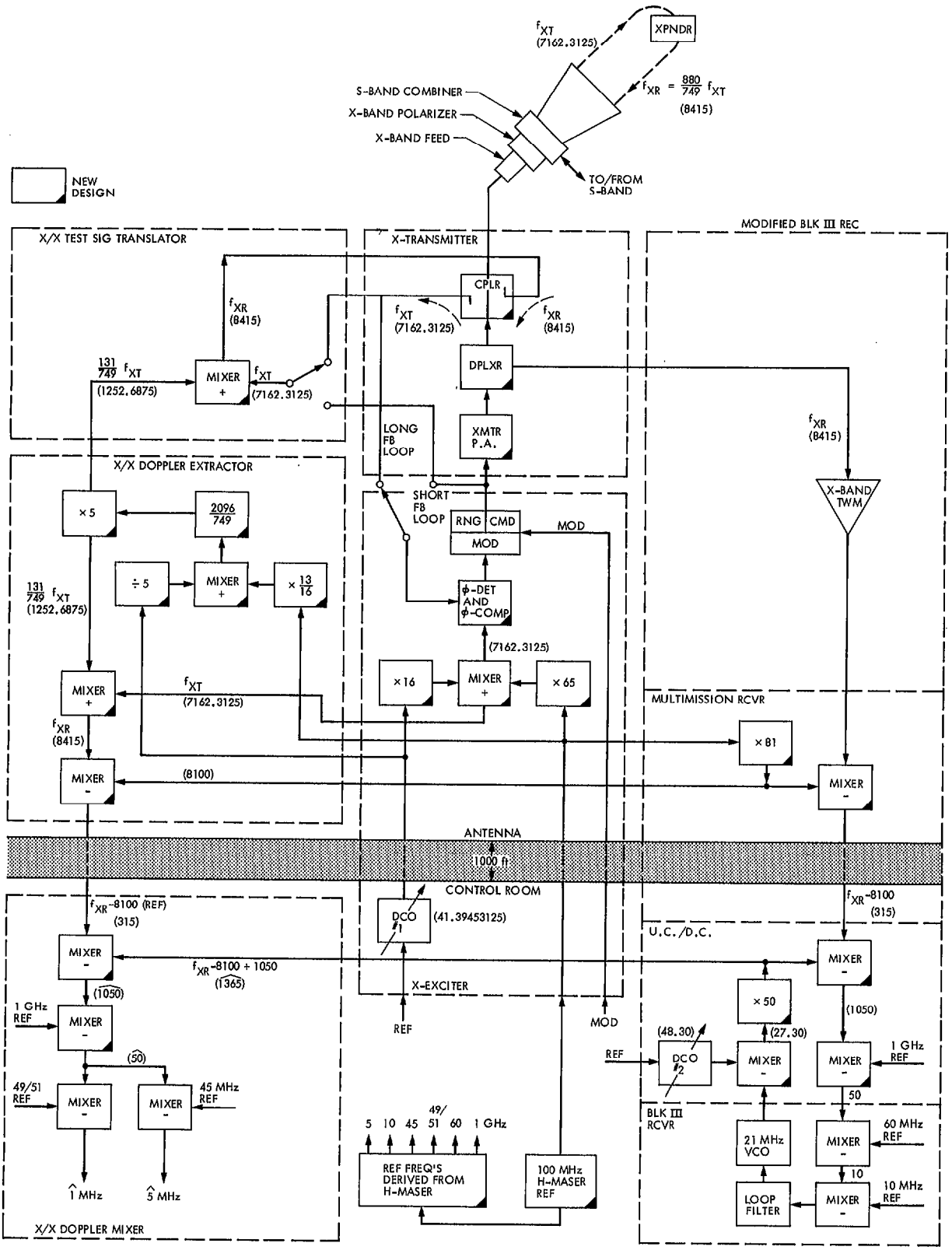

Fig. 2. Detailed functional block diagram for the X-band uplink/X-band downlink hardware at DSS-13 (Example frequencies are for channel 14)

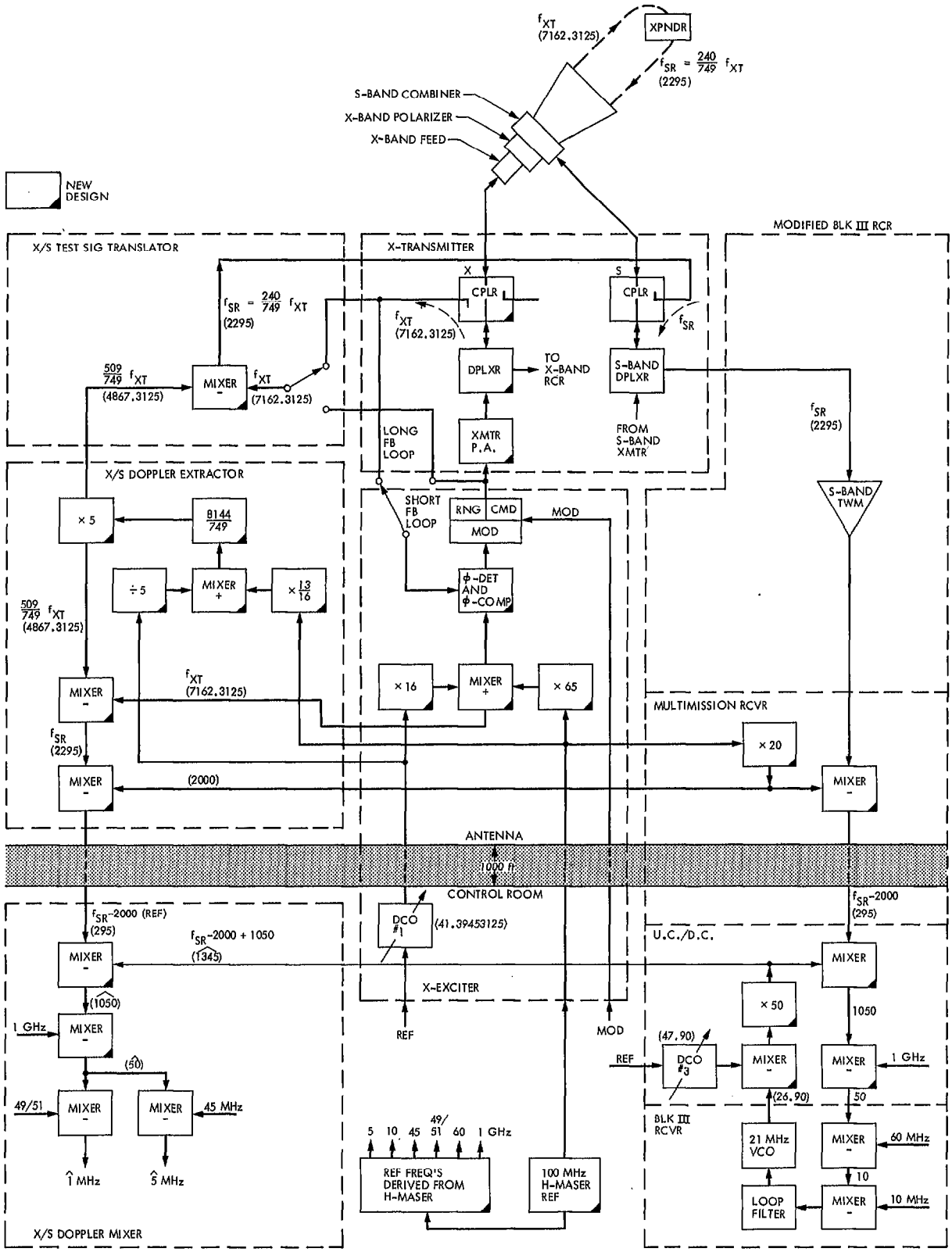

Fig. 3. Detailed functional block diagram for the X-band uplink/S-band downlink hardware at DSS 13 (Example frequencies are for channel 14)

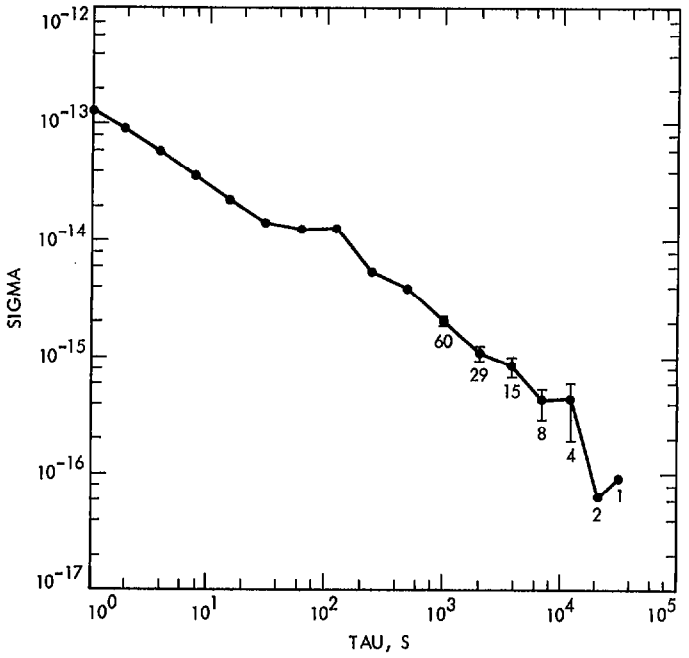

Fig. 4. X-band exciter fractional Allan variance at 7200 MHz, measured at the Interim Frequency Standards Test Facility

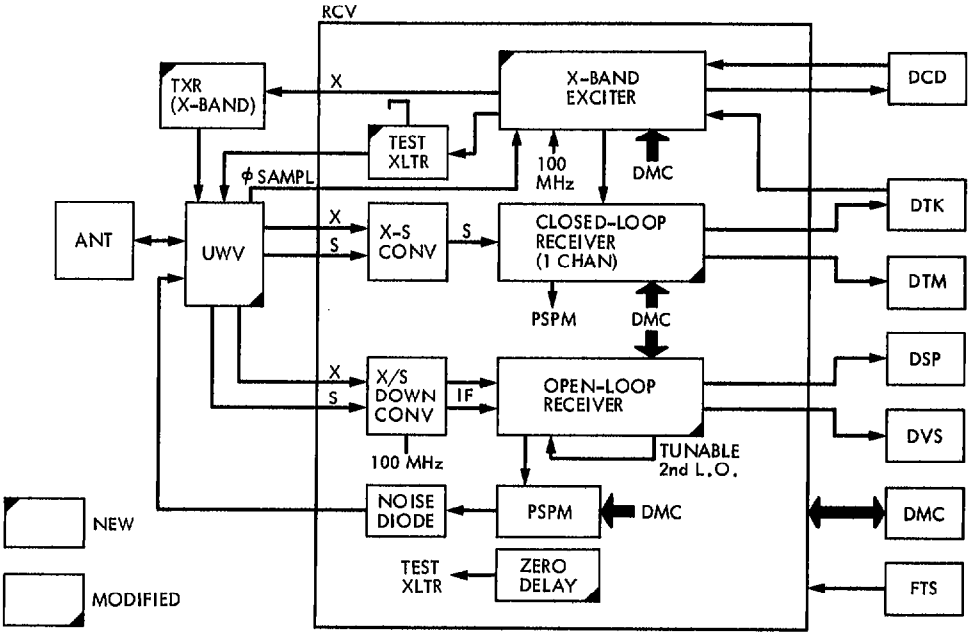

Fig. 5. Functional description block diagram for the 34-M HEF stations